Laser and Particle Beams (2002), *20*, 185–193. Printed in the USA.

DOI: 10.1017/S0263034602202050

Magnetic field effects in strong field ionization of single-electron atoms: Three-dimensional numerical simulations

J.R. VÁZQUEZ DE ALDANA and LUIS ROSO

Departamento de Física Aplicada, Universidad de Salamanca, E-37008 Salamanca, Spain

(Received 15 November 2001; Accepted 18 December 2001)

Abstract

Based on realistic numerical simulations of the three-dimensional time-dependent Schrödinger equation describing a hydrogen atom interacting with a strong electromagnetic field, the influence of the magnetic component is studied. The same computational techniques can be applied to the case of strong field photoionization as well as to the case of ionization by an incident relativistic heavy ion. One of the main consequences, in the strong-laser-field case, is the presence of true even harmonics of the incoming field. In the heavy ion impact, the asymmetry of the wave function reveals the importance of the nondipole nature of the interaction.

Keywords: Magnetic field; Polarized lasers; Single-electron atoms; Strong field ionization; Three-dimensional numerical simulations

1. INTRODUCTION

Strong field ionization of atoms has attracted a lot of interest over the last three decades, mainly due to the availability of short and intense sources (see, e.g., Mainfray & Manus, 1991; Chen *et al.*, 1998; Mourou *et al.*, 1998; Cheriaux & Chambaret, 2001), both from the theoretical and from the experimental points of view (see, e.g., Eberly, 1969; Eberly *et al.*, 1992; Milonni & Sundaram, 1993; Gamaly, 1994; Gibbon, 1997; Protopapas *et al.*, 1997*a*). Some successful theories have been developed to explain the limiting cases (see, e.g., Krstić & Mittleman, 1990; Reiss, 1990, 1996, 2000; Gavrila, 1992; Delone & Krainov, 1993; Geltman, 1994; Joachain *et al.*, 2000; Reiss *et al.*, 1999; San Román *et al.*, 2000). This is particularly true in the high frequency and in the low frequency cases, with convenient approximations. There are, however, many intermediate regions that are unreachable with present day analytical models. Fortunately, computers have extraordinarily increased their speed and memory over the last few years. This opens the door to the *ab initio* study of the ionization dynamics using 3D realistic models.

Address correspondence and reprint requests to: Luis Roso, Departamento de Física Aplicada, Universidad de Salamanca, E-37008 Salamanca, Spain. E-mail: roso@usal.es

2. SUPER INTENSE LASER–ATOM INTERACTIONS

Today, because of the very large clock frequencies reached in processors for personal computers, it is possible to work with fast systems and very large amounts of RAM memory at relatively modest prices. Under certain conditions, the numerical integration of the fully 3D time-dependent Schrödinger equation in a grid can be undertaken with reasonably short computing times and reasonably large numerical grids. Those kinds of strong-field virtual labs started in 1990 (Su *et al.*, 1990) with 1D atoms and soft-core potentials, introducing a grid just along the propagation direction and thus neglecting the influence of the magnetic field. The next step was different 2D models (Dörr *et al.*, 1991; Kulander *et al.*, 1992; Becker *et al.*, 1994; Vivirito & Knight, 1995; Protopapas *et al.*, 1997*b*; Rathe *et al.*, 1997; Patel *et al.*, 1998, 1999*a*, 1999*b*; Hu & Keitel, 1999*a*, 1999*b*, 2001; Kylstra *et al.*, 2000; Ryabikin & Sergeev, 2000; Hu *et al.*, 2001; Vázquez de Aldana *et al.*, 2001), some of them able to include some information on the magnetic field influence.

One of these situations where a fully 3D treatment is required is the photoionization beyond the dipole approximation (Vázquez de Aldana & Roso, 1999). The effect of the magnetic component of a linearly polarized laser field in the interaction with atoms has been previously studied with numerical simulations (Latinne *et al.*, 1994) and ap-

proximated calculations of the 3D nondipole Schrödinger equation (Bugacov *et al.*, 1993; Potvliege, 2000). These calculations rely on expansions of the electronic wave function in a basis of eigenstates.

At that time, it was believed that the onset of relativistic dynamics (electron speeds close to c) would appear much before the onset of magnetic field effects. It seems clear now that there is a region of laser parameters (strong field and high frequency) where the magnetic field component of the pulses appears to be relevant with electron speeds very high but slow enough to be still regarded as nonrelativistic.

With elliptically polarized lasers, no dimensional reduction can be assumed either. In the dipole approximation, an approach of spectral type for numerically integrating the time-dependent Schrödinger equation has been developed in Huens *et al.* (1997). A recent paper studies stabilization in circular polarization (dipole) in 3D grids (Choi & Chism, 2002). However, we have failed to find references to 3D calculations using a circularly polarized laser field without the dipole approximation.

In this section, we discuss how it is possible to solve, in a 3D Cartesian grid, the time-dependent nondipole Schrödinger equation for atomic hydrogen, interacting with very intense and high-frequency laser fields. Both linear and circular polarizations will be considered. Special attention is paid to the effect of the magnetic field component of the laser. The 3D time-dependent Schrödinger equation for a hydrogen atom interacting with a laser field (transverse plane wave) described by $\mathbf{A}(\mathbf{r}, t)$ and with the scalar potential taken to be $\eta = 0$ is:

$$i\hbar \frac{\partial}{\partial t}\Psi(\mathbf{r},t) = \left[-\frac{\hbar^2}{2m}\boldsymbol{\nabla}^2 + \frac{e^2}{2mc^2}A^2(\mathbf{r},t) - \frac{ie\hbar}{mc}\mathbf{A}(\mathbf{r},t)\cdot\boldsymbol{\nabla} + V(r)\right]\Psi(\mathbf{r},t), \tag{1}$$

where $\mathbf{r} = (x, y, z)$ in Cartesian coordinates, and

$$V(r) = -\frac{e^2}{r} = -\frac{e^2}{\sqrt{x^2+y^2+z^2}} \tag{2}$$

is the Coulomb potential. Considering a laser pulse propagating along the x-axis, polarized in the y–z-plane $\mathbf{A}(\mathbf{r}, t) = A_y(x, t)\mathbf{e_y} + A_z(x, t)\mathbf{e_z}$, we can write

$$i\hbar \frac{\partial}{\partial t}\Psi(\mathbf{r},t) = \left[-\frac{\hbar^2}{2m}\left(\frac{\partial^2}{\partial x^2}+\frac{\partial^2}{\partial y^2}+\frac{\partial^2}{\partial z^2}\right) + \frac{e^2}{2mc^2}\mathbf{A}^2(x,t) - \frac{ie\hbar}{mc}A_y(x,t)\frac{\partial}{\partial y} - \frac{ie\hbar}{mc}A_z(x,t)\frac{\partial}{\partial z} - \frac{e^2}{\sqrt{x^2+y^2+z^2}}\right]\Psi(\mathbf{r},t). \tag{3}$$

The spin of the electron is neglected, since it does not contribute at all to the dynamics for the laser parameters considered here (Vázquez de Aldana & Roso, 2002).

This equation is solved in Cartesian coordinates by employing a uniformly sampled grid with $\Delta x = \Delta y = \Delta z = 0.3$ a.u. The numerical technique we use is based on a split-operator method. The wave function at a given time $t + \Delta t$ is calculated from the wave function in the previous time step t by means of the well-known time-evolution operator. It is worth decomposing the exponential in the following way:

$$\begin{aligned}\Psi(\mathbf{r}, t+\Delta t) &\simeq \exp\left[-i\frac{\Delta t}{\hbar}\hat{H}(t+\Delta t/2)\right]\Psi(\mathbf{r},t)\\ &\simeq \exp\left[-i\frac{\Delta t}{2\hbar}\hat{H}_z(t+\Delta t/2)\right]\exp\left[-i\frac{\Delta t}{2\hbar}\hat{H}_x(t+\Delta t/2)\right]\\ &\quad\times\exp\left[-i\frac{\Delta t}{\hbar}\hat{H}_y(t+\Delta t/2)\right]\exp\left[-i\frac{\Delta t}{2\hbar}\hat{H}_x(t+\Delta t/2)\right]\\ &\quad\times\exp\left[-i\frac{\Delta t}{2\hbar}\hat{H}_z(t+\Delta t/2)\right]\Psi(\mathbf{r},t)+O(\Delta t^3),\end{aligned} \tag{4}$$

where $\hat{H}(t)$ is the whole Hamiltonian, and we have defined the following operators:

$$\begin{aligned}\hat{H}_x &= -\frac{\hbar^2}{2m}\frac{\partial^2}{\partial x^2} + \frac{e^2\hbar^2}{2mc^2}A_y^2(x,t) + \frac{e^2\hbar^2}{2mc^2}A_z^2(x,t)\\ \hat{H}_y &= -\frac{\hbar^2}{2m}\frac{\partial^2}{\partial y^2} - \frac{ie\hbar}{mc}A_y(x,t)\frac{\partial}{\partial y} - \frac{e^2}{\sqrt{x^2+y^2+z^2}}\\ \hat{H}_z &= -\frac{\hbar^2}{2m}\frac{\partial^2}{\partial z^2} - \frac{ie\hbar}{mc}A_z(x,t)\frac{\partial}{\partial z}.\end{aligned} \tag{5}$$

The exponentials are thus expressed in the Cayley unitary form, which preserves the norm of the wave function. We employ a Cartesian grid with up to 48×10^6 points, with different sizes and shapes depending on the particular problem considered. The wave function is usually evaluated 500 times per laser cycle and it requires, with our code, approximately 20 h of a single CPU (for a Pentium III 866 MHz node) at the Beowulf cluster (Hargrove *et al.*, 2001) installed in the Optics Group at the University of Salamanca. The accuracy of the numerical technique is expected to lead to maximum errors in the range of 6 to 8%. This estimation has been done by comparing the results obtained for the trajectory computed for a free wave-packet (no Coulomb potential) with classical results (Newton–Lorentz equation).

In the simulations, the electron starts from the ground state, 1s, $\Psi(\mathbf{r}, t = 0) = \psi_{1s}(r)$. This state, computed in a $200 \times 200 \times 200$ grid with the imaginary-time propagation method, overlaps with the analytical ground state of atomic hydrogen better than 99%. The energies obtained for this

https://doi.org/10.1017/S0263034602202050 Published online by Cambridge University Press

state and for a few excited states in that grid are: $E_{1s} = -0.491$ a.u., $E_{2s} = -0.124$ a.u., $E_{2p_{0,\pm1}} = -0.125$ a.u., and $E_{3s} = -0.060$ a.u., in good agreement with theoretical values.

We consider plane–wave laser pulses that propagate along the x-direction and are thus polarized in the y–z-plane. We plan to study both linearly and circularly polarized laser fields. To do so, an ellipticity parameter, ϵ, is introduced. Pulses are described by the electric field:

$$\mathbf{E}(x,t) = E_0 f(x,t)[\sin(kx - \omega_L t)\mathbf{e}_y + \epsilon \cos(kx - \omega_L t)\mathbf{e}_z], \tag{6}$$

where $f(x,t)$ is the pulse envelope and $k = \omega_L/c$. Retardation is also included in the envelope (i.e., the envelope is a function of $x - ct$). We consider two polarization states: $\epsilon = 0$ for a linearly polarized pulse and $\epsilon = 1$ for a circularly polarized one. The vector potential is computed from the electric field by means of

$$\mathbf{A}(x,t) = -c \int_0^t \mathbf{E}(x,t')\, dt'. \tag{7}$$

(The scalar potential is taken to be zero.) The validity of employing propagating electromagnetic fields, that is, Lorentz-invariant fields, with a nonrelativistic wave equation, Galilean-invariant equation, does not constitute a major problem for the frequency and intensity considered throughout this section. Laser frequency is $\omega_L = 1$ a.u. (corresponding to an ultraviolet photon energy of 27.2 eV, and a wavelength of 45.6 nm). We have selected an amplitude of $E_0 = 15$ a.u. (intensity $I_0 = 7.9 \times 10^{18}$ W/cm^2 for the linearly polarized pulse and $I_0 = 1.6 \times 10^{19}$ W/cm^2 for the circularly polarized one). With this choice of wavelength and intensity, we reach a region where the electric-dipole approximation in the Schrödinger equation fails, and a large displacement of the electron wave-packet in the propagation direction appears. It is caused by the coupling of the magnetic field component and the velocity achieved by the electron in the field (Sarachik & Schappert, 1970; Keitel & Knight, 1995; Urbach & Keitel, 2000). The intensity selected represents a compromise between the failure of the dipole approximation and the onset of relativistic dynamics.

Considering a long pulse involves the problem that the ionized population reaches the boundaries of the integration box, and some kind of absorbing mask must be employed in order to avoid reflections. When absorbing boundaries are used, the norm of the wave function decreases artificially and it is therefore not possible to compute expectation values of physical magnitudes (operators) that do not vanish in the vicinity of the origin.

We first simulate a linearly polarized pulse ($\epsilon = 0$) with a trapezoidal envelope. The envelope $f(x,t)$ includes retardation and the turn-on lasts 4 cycles. Note that we have not included the turn-off of the pulse because we will only compute the wave function during the turn-on and some cycles at the constant intensity part until the amount of population reaching the absorbing boundaries makes the simulation unrealistic. In Figure 1 we show snapshots of the wave function at a time equal to 9.5 cycles (4 cycles ramp plus 5.5 cycles of constant amplitude). The contour plots represent slices of the electronic probability density at the $z = 0$ (upper plot), $y = 0$ (middle plot), and $x = 0$ (lower plot) planes. Contour lines are in linear scale. It should be noted that the magnetic drift is in the positive direction of the x axis. The effect of the magnetic field is clearly observed in this drawing. In the dipole approximation, it would have been symmetrical with respect to the $x = 0$ plane.

Now, let us consider a circularly polarized pulse $\epsilon = 1$, with the same laser parameters as above. Contour plots in Figure 2 are similar to the previous figure. The laser pulse has a 4-cycle linear turn-on and then a constant envelope.

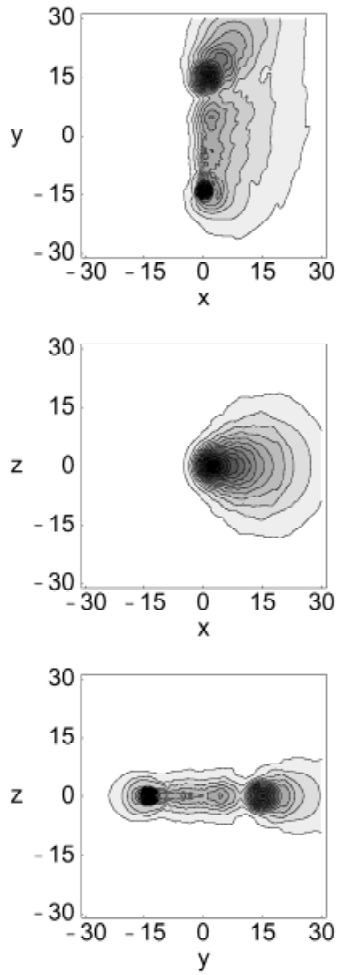

Fig. 1. Atomic hydrogen interacting with a linearly polarized laser field. The contour plots are slides of the probability density at the planes $z = 0$ (plot at the top), $y = 0$ (plot in the middle), and $x = 0$ (plot at the bottom), and the contour lines are in linear scale. The laser pulse has a 4-cycle linear turn-on and then a constant envelope part: The snapshot was taken at $t = 9.5$ T. The amplitude of the laser is $E_0 = 15$ a.u. and the frequency is $\omega_L = 1$ a.u.

https://doi.org/10.1017/S0263034602202050 Published online by Cambridge University Press

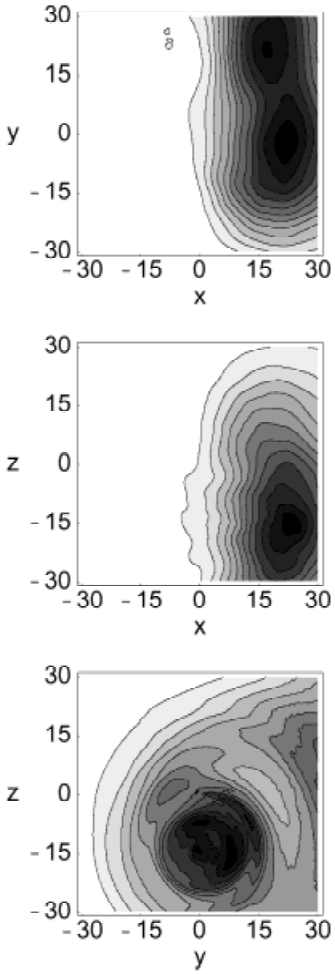

Fig. 2. Atomic hydrogen interacting with a circularly polarized laser field. The contour plots are slides of the probability density at the planes $z = 0$ (plot at the top), $y = 0$ (plot in the middle), and $x = 0$ (plot at the bottom), and the contour lines are in linear scale. The laser pulse has a 4-cycle linear turn-on and then a constant envelope part: The snapshot was taken at $t = 8.5$ T. The amplitude of the laser is $E_0 = 15$ a.u. and the frequency is $\omega_L = 1$ a.u.

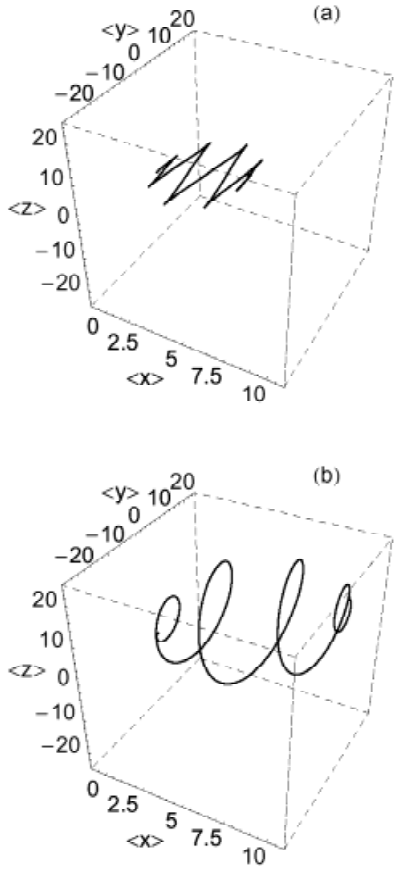

Fig. 3. Parametric plot of the expectation value of the electron's trajectory for the linearly polarized laser pulse (a) and for the circularly polarized one (b). The pulse has a 6-cycles $\sin^2$ envelope. The amplitude of the laser is $E_0 = 15$ a.u. and the frequency is $\omega_L = 1$ a.u.

The snapshot is taken at time equal to 8.5 cycles. Of course, the window of the plot is much narrower that the size of the grid. The dynamics of the electron in the circularly polarized case is very peculiar: Because of the very high intensity of the laser, the electron is almost released during the first few cycles of the interaction. As the laser becomes more and more intense, the helicoidal trajectory of the electron (that now behaves nearly as free) pushes it far from the nucleus, and the interaction with the nucleus is very small.

Figure 3 shows the expectation value of the electron's trajectory. In this case, the pulse duration is taken to be 6 optical cycles, with a $\sin^2$ envelope. Using this ultrashort pulse, almost no population reaches the boundaries of the integration grid at the end of the pulse. Thus, we do not need to employ any absorbing mask close to the boundaries, and expected values can be safely computed with no artificial change in the norm of the wave function. The nonnegligible dynamics in the longitudinal direction will lead to an appreciable contribution to the radiation emitted by the electron with this polarization. From the expectation value of the position operator, the spectrum of the radiation emitted by the electron can be computed. The far field is given by (see, e.g., Jackson, 1998)

$$\mathbf{E} = \frac{e}{c}\left[\frac{\mathbf{n}\times(\mathbf{n}\times\mathbf{a})}{cR}\right]_{ret}, \tag{8}$$

where $\mathbf{a}$ is the acceleration of the electron. This expression is directly computed from $\mathbf{a} = d^2\langle\mathbf{r}\rangle/dt^2$. We compute the intensity of the radiation emitted in the longitudinal direction, $\mathbf{n} = (1,0,0)$. By performing a Fourier transform, we calculate the radiated spectrum, shown in Figure 4 for the case of linear polarization. This direction is relevant to understand the magnetic field effects because in the dipole approximation the radiation in this direction vanishes. This emission evidences a motion along the longitudinal direction that has components at twice the fundamental frequency. Therefore even-order harmonics appear. Observe that for this direction, even-order harmonics dominate the radiation spectrum.

https://doi.org/10.1017/S0263034602202050 Published online by Cambridge University Press

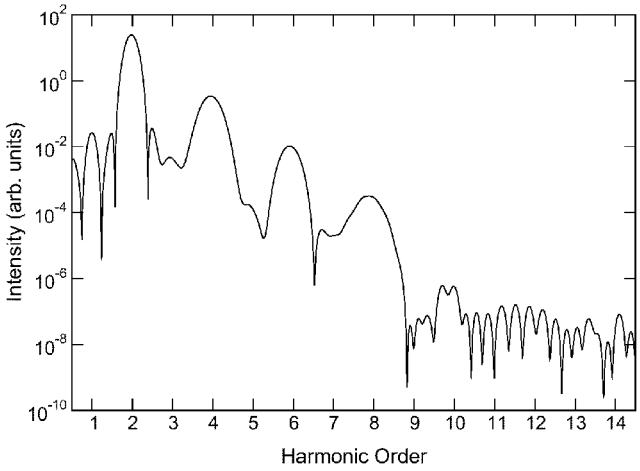

Fig. 4. Spectrum of the radiation emitted with polarization along the propagation direction (x-axis). Such radiation is not present in the dipole approximation. Dominance of the even harmonics results from the motion in the longitudinal direction induced by the magnetic field. The spectrum corresponds to the same parameters as the electronic expectation trajectory shown in Figure 3: The pulse has a 6-cycles $\sin^2$ envelope, the peak amplitude $E_0 = 15$ a.u., and the frequency is $\omega_L = 1$ a.u.

Let us remark that in the electric dipole approximation, a hydrogen atom in the ground state interacting with a truly optical laser pulse, $\langle E(t)\rangle = 0$, does not emit even harmonics due to parity and symmetry considerations. There are, however, certain spectral lines that under given circumstances will lie close to the position of the even harmonics, but these emission lines should not be interpreted as harmonics. The same result holds for molecules. For example, in the electric dipole approximation, the H_2 molecule does not generate even harmonics, while the HD molecule does (Kreibich *et al.*, 2001).

The existence of even harmonics, along the longitudinal direction (as shown in Fig. 4) as well as along the laser polarization direction (not shown in this article) evidences the influence of the magnetic field component and the oscillation that it induces at twice the fundamental frequency. The fully 3D treatment is thus required for certain range of laser parameters.

3. RELATIVISTIC HEAVY-ION IMPACT AGAINST ATOMIC HYDROGEN

Atomic ionization due to an electromagnetic wave, either incoherent or coherent, has been widely studied since the old times of Quantum Mechanics in many different situations. However, it is also possible but much less common in this context, to study ionization by the electromagnetic fields generated by a fast charged projectile passing nearby. In the case of a laser field, or indeed of any other electromagnetic wave, the field is a radiation field far from the sources; in other words, it is made of real photons. However, in the case of a rapidly passing projectile, the field has different properties and is made of virtual photons.

It is clear that such virtual photons can ionize the atom, but the ionization dynamics should be quite different from the laser field case. Recently, considerable interest has been devoted to this subject (Burgdörfer *et al.*, 1994; Wang *et al.*, 1996; Stolterfoht *et al.*, 1998), both for single and multiple ionization of atoms with fast ions. However, very few experiments have been reported with relativistic incident ions. At the GSI in Darmstadt (Moshammer *et al.*, 1997), experiments with relativistic incident ions have been performed. The GSI experiments studied the single and double ionization of helium by 1 GeV/nucleon U^{92+} impact. As the authors state, the relativistic ion generates a subattosecond superintense electromagnetic pulse that is more similar to a "kick" than to an oscillating wave. It has a maximum that only lasts for a very short time with long wings due to the long range of the Coulomb potential. That pulse has some common features with half-cycle pulses (Reinhold & Burgdörfer, 1995; Reinhold *et al.*, 1996). However, when the impact parameter of the ion is short enough to cross over the electronic wave function, the strong space dependence of the fields will lead to a dynamics of the electron very different from the laser pulse case. Some of these features will be analyzed in this section, for U^{92+} colliding against atomic hydrogen at 1 GeV/nucleon.

Due to the geometry of the system (incident projectile and nucleus), there are no symmetries present except for a mirror symmetry along the plane defined by the projectile trajectory and the initial position of the nucleus. Therefore, 3D studies are needed and this is extremely difficult to carry out *ab initio* for a two-electron system. In the present work, we offer a very realistic description of the ion–atom interaction but just for one-electron atoms. We compute the electron wave function in a Cartesian 3D lattice, taking into account the relativistic dynamics of the projectile.

Calculations in 3D Cartesian grids have been shown to be a very good description for $p + H$ collisions (Gavras *et al.*, 1995; Kolakowska *et al.*, 1998, 1999; Schultz *et al.*, 1999) and $p + He^+$ (Tong *et al.*, 2001) with nonrelativistic incident protons. The agreement with the experimental results is remarkably good for the range of parameters considered. Collisions with antiprotons have also been investigated with these simulations (Schultz *et al.*, 1996, 1997; Wells *et al.*, 1996). However, these calculations are done in a context that is not able to describe the peculiar features of the electromagnetic fields (electric and magnetic fields) generated by the relativistically moving projectile. To our knowledge, no previous studies have been performed based on the direct numerical resolution of the wave equation in cases where the incident ion is relativistic.

To proceed with this simulation, we first need to calculate the electromagnetic field generated by the relativistic ion. As our particular choice of coordinates, in order to simplify the notation without loss of generality, we consider that the heavy ion projectile is moving in the plane $z = 0$ in a direction parallel to the x-axis. The hydrogen nucleus is initially at the origin and the projectile trajectory is $X(t) = X_0 + vt =$

https://doi.org/10.1017/S0263034602202050 Published online by Cambridge University Press

$X_0 + \beta ct$, $Y(t) = b$ and $Z(t) = 0$. b is the impact parameter (minimum distance to the nucleus in the trajectory of the ion). The notation $\beta = v/c$ is standard in relativity. The projectile is so heavy ($M_{ion} = 238 m_N$, m_N being the nucleon mass) and so energetic that we can perfectly assume that its trajectory is not affected by the atom. It is not difficult to show (see, e.g., Jackson, 1998) that the electric and magnetic fields created by such a relativistic projectile at an arbitrary point (x, y, z) of space are

$$\mathbf{E}(\mathbf{r}, t) = \frac{Ze\gamma}{[\gamma^2(x - X_0 - vt)^2 + (y - b)^2 + z^2]^{3/2}} \times [(x - X_0 - vt), y, z] \tag{9}$$

and

$$\mathbf{B}(\mathbf{r}, t) = \frac{-Ze\gamma^3 v/c}{[\gamma^2(x - X_0 - vt)^2 + (y - b)^2 + z^2]^{3/2}} (0, z, -y), \tag{10}$$

with $\gamma = 1/\sqrt{1 - \beta^2}$. Z indicates the projectile ion charge, which in the case studied here is $Z = 92$. These fields are generated by a scalar potential

$$\eta(\mathbf{r}, t) = \frac{Ze\gamma}{\sqrt{\gamma^2(x - X_0 - vt)^2 + (y - b)^2 + z^2}} \tag{11}$$

and a vector potential

$$\mathbf{A}(\mathbf{r}, t) = \frac{Ze\gamma \mathbf{v}/c}{\sqrt{\gamma^2(x - X_0 - vt)^2 + (y - b)^2 + z^2}}. \tag{12}$$

The velocity vector has only one component, $\mathbf{v} = (v, 0, 0)$ and hence $\mathbf{A}(\mathbf{r}, t) = A_x(\mathbf{r}, t)\mathbf{e}_x$ and $A_y = A_z = 0$.

In our study, we are able to give a quantum description of the dynamics of the atomic electron interacting with the ion. However, we have also performed some classical Monte Carlo simulations for the motion of the projectile ion, the proton, and the electron. The goal of such simulations is just to introduce the right approximations for the subsequent quantum description. Some conclusions can be drawn from the classical simulations for heavy projectiles (U^{92+}) that move relativistically (1 GeV/nucleon, or more). First, the projectile trajectory is not changed at the space scale and with the precision in which we are interested. Second, the hydrogen nucleus is accelerated after the collision with the projectile, but the momentum transfer is negligible unless we consider impact parameters smaller than 0.1 a.u. We are not interested in head-on collisions, although these could relevant for nuclear physics. One result is clear: To study ionization up to the level of accuracy in which we are interested, it is fairly exact to consider that the projectile ion follows its trajectory unaltered. It is also reasonable, because of the short interaction time, to consider that the hydrogen nucleus remains unaltered at its initial position. Therefore, only the electron motion needs to be described in detail. Moreover, except for very small impact parameters, the dynamics of the electron remains nonrelativistic, and a nonrelativistic wave equation to describe the interaction of the atom with the ion is thus justified. Because the electron is interacting with such time- and space-dependent scalar and vector potentials, the correct nonrelativistic spinless wave equation is

$$i\hbar \frac{\partial \Psi}{\partial t} = \frac{\mathbf{p}^2}{2m} \Psi + \frac{e}{mc} \mathbf{A} \cdot \mathbf{p} \Psi + \frac{e^2}{2mc^2} \mathbf{A}^2 \Psi - e\eta \Psi - eV \Psi - i \frac{e\hbar}{2mc} \left(\boldsymbol{\nabla} \cdot \mathbf{A} + \frac{1}{c} \frac{\partial \eta}{\partial t} \right) \Psi. \tag{13}$$

(A similar equation can be seen in Greiner (1997). To our knowledge, not exhaustive, this is the only textbook that mentions the need for the time derivative of the scalar potential.) Because the scalar and vector potentials verify the Lorentz gauge condition,

$$\boldsymbol{\nabla} \cdot \mathbf{A} + \frac{1}{c} \frac{\partial \eta}{\partial t} = 0, \tag{14}$$

the wave equation is much simplified. Note that this equation is different from the standard time-dependent Schrödinger equation, which considers the term $(c\mathbf{p} + e\mathbf{A})^2$: It includes the divergence of the vector potential but does not include the very important $i\partial\eta/\partial t$ term. Such an equation is not general and cannot be safely employed to describe the interaction with arbitrary electromagnetic fields. Only transversal electromagnetic fields can be described accurately. The derivation of Eq. (13) will be given elsewhere.

Another important point to clarify for the correctness of our model is the following. The fields that we describe with $\mathbf{A}$ and η, Eq. (11) and Eq. (12), are invariant under Lorentz transformations and, on the contrary, the time-dependent Schrödinger equation is invariant under Galilean transformations due to its nonrelativistic nature. Fortunately, this formal inconsistency in our model is not important (from the practical point of view) if the dynamics of the electron is nonrelativistic, and hence Lorentz transformations reduce to Galilean transformation (in the low velocity regime).

The final equation that we consider is

$$i\hbar \frac{\partial \Psi(\mathbf{r}, t)}{\partial t} = -\frac{\hbar^2}{2m} \boldsymbol{\nabla}^2 \Psi(\mathbf{r}, t) - i \frac{e\hbar}{mc} \mathbf{A}(\mathbf{r}, t) \cdot \boldsymbol{\nabla} \Psi(\mathbf{r}, t) + \frac{e^2\hbar^2}{2mc^2} \mathbf{A}(\mathbf{r}, t)^2 \Psi(\mathbf{r}, t) - e\eta(\mathbf{r}, t)\Psi(\mathbf{r}, t) - eV(\mathbf{r})\Psi(\mathbf{r}, t). \tag{15}$$

https://doi.org/10.1017/S0263034602202050 Published online by Cambridge University Press

$V(\mathbf{r})$ is the Coulomb potential of the hydrogen nucleus. The electromagnetic potentials are given by Eqs. (11) and (12), and they already satisfy the Lorentz condition because they come from the Lorentz transform of a Coulomb potential.

We solve Eq. (15) with the same kind of algorithms that were described for the laser–atom interaction (Eq. 1) with slight modifications. The time-evolved wave function is computed from

$$\begin{aligned}\Psi(\mathbf{r}, t+\Delta t) &\simeq \exp\left[-i\frac{\Delta t}{\hbar}\hat{H}(t+\Delta t/2)\right]\Psi(\mathbf{r},t)\\ &\simeq \exp\left[-i\frac{\Delta t}{2\hbar}\hat{H}_z(t+\Delta t/2)\right]\exp\left[-i\frac{\Delta t}{2\hbar}\hat{H}_y(t+\Delta t/2)\right]\\ &\times \exp\left[-i\frac{\Delta t}{\hbar}\hat{H}_x(t+\Delta t/2)\right]\exp\left[-i\frac{\Delta t}{2\hbar}\hat{H}_y(t+\Delta t/2)\right]\\ &\times \exp\left[-i\frac{\Delta t}{2\hbar}\hat{H}_z(t+\Delta t/2)\right]\Psi(\mathbf{r},t)+O(\Delta t^3). \qquad (16)\end{aligned}$$

We have now defined the Hamiltonian operators as follows:

$$\begin{aligned}\hat{H}_x &= -\frac{\hbar^2}{2m}\frac{\partial^2}{\partial x^2}+\frac{e^2\hbar^2}{2mc^2}\mathbf{A}(\mathbf{r},t)^2 - i\frac{e\hbar}{mc}A_x(\mathbf{r},t)\frac{\partial}{\partial x}\\ &\quad - e\eta(\mathbf{r},t) - eV(\mathbf{r})\\ \hat{H}_y &= -\frac{\hbar^2}{2m}\frac{\partial^2}{\partial y^2}, \qquad \hat{H}_z = -\frac{\hbar^2}{2m}\frac{\partial^2}{\partial z^2}. \qquad (17)\end{aligned}$$

The numerical procedure from this point is nearly the same that for the laser–atom interaction.

In our calculations, absorbers (a mask function) were employed at the integration boundaries in order to avoid reflections of the ionized population. The mask function has the form $\sin^{1/8}$ and is applied over 40 points along the edge of the grid. However, the interaction time is short enough to prevent a very large amount of the population reaching the boundaries (the absorbed population is always smaller that 1%). It has also been checked that the absorbed population hardly changes when the mask is applied over 30 or 50 points. The step size is again $\Delta x = \Delta y = \Delta z = 0.3$ a.u.

The hydrogen nucleus is placed at the origin of the Cartesian coordinates. For the energy of the incident ion chosen (1 GeV/nucleon), the relativistic parameters are $\beta = 0.3696$ and $\gamma = 1.076$. The U^{92+} nucleus is initially at $X(0) = X_0 = -200$ a.u., $X(0) = b$, and $X(0) = 0$ a.u. This choice of the initial value of $X(0)$ is a good compromise between accuracy—due to the long range of the Coulomb potential—and a reasonable computer time. The electronic wave function is propagated in time until the ion reaches $X(\tau) = 600$ a.u. ($\tau = 15.8$ a.u. is the final time). We employ 2667 time iterations, so that the ion covers a distance equal to the grid spacing (0.3 a.u.) each time step ($\Delta t = \Delta x/v = 0.00592$ a.u.). To avoid problems with the singularity of the Coulomb potential of the ion, the projectile moves equidistantly to the nearest points of the lattice.

An example of the impact of U^{92+} against atomic hydrogen with $b = 5$ a.u. is shown in Figure 5. Contour plots represent the probability density at different times of the interaction with the ion, at the planes $z = 0$ (plots at the top), $y = 0$ (plots in the middle), and $x = 0$ (plots at the bottom). The column on the left corresponds to the time at which the ion is placed at the minimum distance to the nucleus $[X_{ion}(t) = 0]$. At this time, the wave function is slightly distorted, but the acceleration of the electrons reach the maximum. The column in the middle corresponds to $X_{ion}(t) = 236$ a.u. ($t = 6.9$ a.u.) and the column on the right for $X_{ion}(t) = 472$ a.u. ($t = 12.6$ a.u.). The contour lines are in logarithmic scale. In the frame $z = 0$ in the first column, the effect of the incident ion can be observed as a distortion of the wave packet, that crosses over the electron wave function. Once the projectile has passed, the ionized population mainly moves along the transverse direction (y-axis), but a clear asymmetry in the wave packet caused by the strong nondipole interaction can be seen.

4. CONCLUSIONS

Three-dimensional numerical simulations constitute an excellent tool to investigate magnetic field effects on the ionization of single electron atoms. A few years ago, such simulations, within realistic conditions, were restricted to supercomputer centers. Today the cheap price of ordinary PC computers, together with the possibilities opened by Linux OS, allows a new strategy: the Beowulf-type Linux clusters.

Our numerical simulations are based on the time-dependent Schrödinger equation, with some specifications for nonsolenoidal vector potentials. The present simulations show that the magnetic field effects are present before the onset of relativistic dynamics. There are certain regions of parameters where the Lorentz force is important but the relativistic dynamics is not strictly necessary. Regardless of our interest in magnetic fields, spin effects are meaningless. We have repeated some of the calculations using the Pauli wave equation, instead of the spinless Schrödinger equation, without finding any observable effect of the spin, to the accuracy of our numerical codes.

We have presented here simulations for the photoionization with a high frequency strong field laser pulse. Those realistic simulations evidence the appearance of even harmonics of the incident field induced by the magnetic component of the Lorentz force at twice the laser frequency. As even harmonics are not allowed in the dipole approximation, those results can be regarded as a possible experimental clue for the onset of magnetic field drifts.

We have also presented results for the impact ionization using a fast heavy-ion projectile. In this case, ionization is

https://doi.org/10.1017/S0263034602202050 Published online by Cambridge University Press

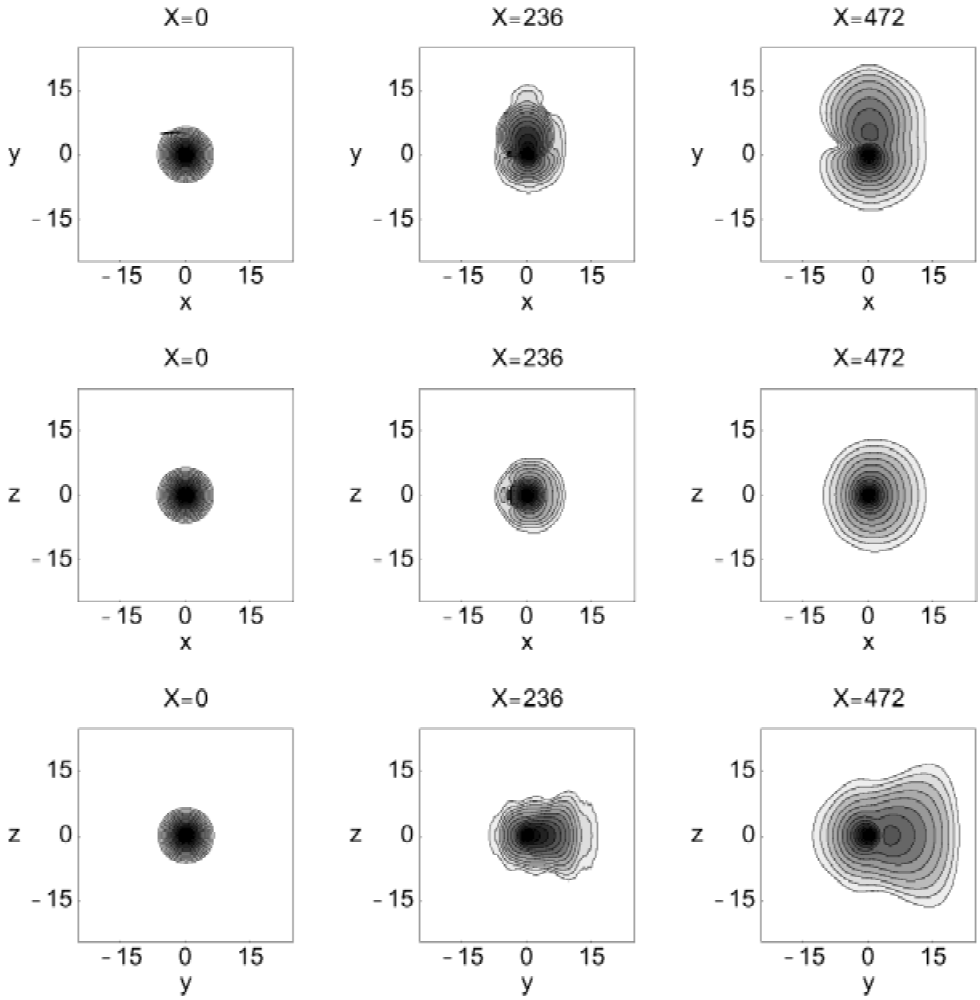

Fig. 5. Impact of U^{92+} against atomic hydrogen with $b = 5$ a.u. In the plots, we show the probability density in the planes $z = 0$ (top), $y = 0$ (middle), and $x = 0$ (bottom) at different times of the interaction with the ion. The position of the ion appears at the top of each plot.

due to an electromagnetic field and not to an electromagnetic wave, that is, longitudinal fields also appear, that evidence the need for 3D simulations.

ACKNOWLEDGMENTS

This work has been partially supported by the Spanish Dirección General de Enseñanza Superior e Investigación Científica (grant PB98-0268) and by the Junta de Castilla y León and Unión Europea, FSE (grant SA044/01). We thank Dr. M.A. Matías for his inestimable assistance in setting up the Beowulf Linux cluster and other computers in the group of Salamanca. Fruitful discussions related to programming techniques and computing tasks with C.M. Valverde are also acknowledged.

REFERENCES

Becker, W., Long, S. & McIver, J.K. (1994). *Phys. Rev. A* **50**, 1540.

Bugacov, A., Pont, M. & Shakeshaft, R. (1993). *Phys. Rev. A* **48**, R4027.

Burgdörfer, J., Anderson, L.R., McGuire, J.H. & Ishihara, T. (1994). *Phys. Rev. A* **50**, 349.

Chen, S., Maksimchuk, A. & Umstadter, D. (1998). *Nature* **396**, 653.

Cheriaux, G. & Chambaret, J.-P. (2001). *Meas. Sci. Technol.* **12**, 1769.

Choi, D. & Chism, W. (2002). *Phys. Rev. A* **66**, 025401.

Delone, N.B. & Krainov, V.P. (1993). *Multiphoton Processes in Atoms.* Berlin: Springer-Verlag.

Dörr, M., Potvliege, R.M., Proulx, D. & Shakeshaft, R. (1991). *Phys. Rev. A* **43**, 3729.

Eberly, J.H. (1969). *Prog. Opt*. vol. 7, p. 359. Amsterdam: North-Holland.

Eberly, J.H., Grobe, R., Law, C.K. & Su, Q. (1992). *Atoms in Intense Laser Fields* (Gavrila, M., Ed.) p. 301. New York: Academic Press.

Gamaly, E.G. (1994). *Laser Part. Beams* **12**, 185.

https://doi.org/10.1017/S0263034602202050 Published online by Cambridge University Press

Gavras, P., Pindzola, M.S., Schultz, D.R. & Wells, J.C. (1995). *Phys. Rev. A* **52**, 3868.
Gavrila, M. (1992). *Atoms in Intense Laser Fields* (Gavrila, M., Ed.) p. 435. New York: Academic Press.
Geltman, S. (1994). *J. Phys. B: At. Mol. Opt. Phys.* **27**, 257.
Gibbon, P. (1997). *IEEE J. Quantum Electron.* **33**, 1915.
Greiner, W. (1997). *Quantum Mechanics*. Berlin: Springer.
Hargrove, W.W., Hoffman, F.M. & Sterling, T. (2001). The Do-It-Yourself Supercomputer. *Sci. Am.* **265**(2), 72–79.
Hu, S.X. & Keitel, C.H. (1999*a*). *Europhys. Lett.* **47**, 318.
Hu, S.X. & Keitel, C.H. (1999*b*). *Phys. Rev. Lett.* **83**, 4709.
Hu, S.X. & Keitel, C.H. (2001). *Phys. Rev. A* **63**, 053402.
Hu, S.X., Milosevic, D.B., Becker, W. & Sandner, W. (2001). *Phys. Rev. A* **64**, 013410.
Huens, E., Piraux, B., Bugacov, A. & Gadja, M. (1997). *Phys. Rev. A* **55**, 2132.
Jackson, J.D. (1998). *Classical Electrodynamics*. New York: John Wiley & Sons.
Joachain, C.J., Dörr, M. & Kylstra, N.J. (2000). *Adv. At. Mol. Opt. Phys.* **42**, 225.
Keitel, C.H. & Knight, P.L. (1995). *Phys. Rev. A* **51**, 1420.
Kolakowska, A., Pindzola, M.S., Robicheaux, F., Schultz, D.R. & Wells, J.C. (1998). *Phys. Rev. A* **58**, 2872.
Kolakowska, A., Pindzola, M.S. & Schultz, D.R. (1999). *Phys. Rev. A* **59**, 3598.
Kreibich, T., Lein, M., Engel, V. & Gross, E.K.U. (2001). *Phys. Rev. Lett.* **87**, 103901.
Krstić, P.S. & Mittleman, M.H. (1990). *Phys. Rev. A* **42**, 4037.
Kulander, K.C., Schafer, K.J. & Krause, J.L. (1992). *Atoms in Intense Laser Fields* (Gavrila, M., Ed.) p. 207. New York: Academic Press.
Kylstra, N.J., Worthington, R.A., Patel, A., Knight, P.L., Vázquez de Aldana, J.R. & Roso, L. (2000). *Phys. Rev. Lett.* **85**, 1835.
Latinne, O., Joachain, C.J. & Dörr, M. (1994). *Europhys. Lett.* **26**, 333.
Mainfray, G. & Manus, C. (1991). *Rep. Prog. Phys.* **54**, 1333.
Milonni, P.W. & Sundaram, B. (1993). *Prog. Opt.* **33**, 1.
Moshammer, R., Schmitt, W., Ullrich, J., Kollmus, H., Cassimi, A., Dörner, R., Jagutzki, O., Mann, R., Olson, R.E., Prinz, H.T., Schmidt-Böcking, H. & Spielberg, L. (1997). *Phys. Rev. Lett.* **79**, 3621.
Mourou, G.A., Barty, Ch.P.J. & Perry, M.D. (1998). *Phys. Today* **Jan.** 22.
Patel, A., Kylstra, N.J. & Knight, P.L. (1999*a*). *Opt. Express* **4**, 496.
Patel, A., Kylstra, N.J. & Knight, P.L. (1999*b*). *J. Phys. B: At. Mol. Opt. Phys.* **32**, 5759.
Patel, A., Protopapas, M., Lappas, D.G. & Knight, P.L. (1998). *Phys. Rev. A* **58**, R2652.
Potvliege, R.M. (2000). *Laser Phys.* **10**, 143.
Protopapas, M., Keitel, C.H. & Knight, P.L. (1997*a*). *Rep. Prog. Phys.* **60**, 389.
Protopapas, M., Lappas, D.G. & Knight, P.L. (1997*b*). *Phys. Rev. Lett.* **79**, 4550.
Rathe, U.W., Keitel, C.H., Protopapas, M. & Knight, P.L. (1997). *J. Phys. B: At. Mol. Phys.* **11**, L531.
Reinhold, C.O. & Burgdörfer, J. (1995). *Phys. Rev. A* **51**, R3410.
Reinhold, C.O., Burgdörfer, J., Frey, M.T. & Dunning, F.B. (1996). *Phys. Rev. A* **54**, R33.
Reiss, H.R. (1990). *J. Opt. Soc. Am. B* **7**, 574.
Reiss, H.R. (1996). *J. Opt. Soc. Am. B* **13**, 355.
Reiss, H.R. (2000). *Phys. Rev. A* **63**, 013409.
Reiss, H.R., Shabaev, A. & Wang, H. (1999). *Laser Phys.* **9**, 92.
Ryabikin, M.Yu. & Sergeev, A.M. (2000). *Opt. Express* **7**, 217.
San Román, J., Roso, L. & Reiss, H.R. (2000*). J. Phys. B: At. Mol. Opt. Phys.* **33**, 1869.
Sarachik, E.S. & Schappert, G.T. (1970). *Phys. Rev. D* **1**, 2738.
Schultz, D.R., Krstić, P.S., Reinhold, C.O. & Wells, J.C. (1996). *Phys. Rev. Lett.* **76**, 2882.
Schultz, D.R., Strayer, M.R. & Wells, J.C. (1999). *Phys. Rev. Lett.* **82**, 3976.
Schultz, D.R., Wells, J.C., Krstić, P.S. & Reinhold, C.O. (1997). *Phys. Rev. A* **56**, 3710.
Stolterfoht, N., Chesnel, J.-Y., Grether, M., Skogvall, B., Frémont, F., Lecler, D., Hennecart, D., Husson, X., Grandin, J.P., Sulik, B., Gulyás, L. & Tanis, T.A. (1998). *Phys. Rev. Lett.* **80**, 4649.
Su, Q., Eberly, J.H. & Javanainen, J. (1990). *Phys. Rev. Lett.* **64**, 862.
Tong, X.M., Watanabe, T., Kato, D. & Ohtani, S. (2001). *Phys. Rev. A* **64**, 022711.
Urbach, D.J. & Keitel, C.H. (2000). *Phys. Rev. A* **61**, 043409.
Vázquez de Aldana, J.R., Kylstra, N.J., Roso, L., Knight, P.L., Patel, A. & Worthington, R.A. (2001). *Phys. Rev. A* **64**, 013411.
Vázquez de Aldana, J.R. & Roso, L. (1999). *Opt. Express* **5**, 144.
Vázquez de Aldana, J.R. & Roso, L. (2000). *J. Phys. B: At. Mol. Opt. Phys.* **33**, 3701.
Vivirito, R.M.A. & Knight, P.L. (1995). *J. Phys. B: At. Mol. Opt. Phys.* **28**, 4357.
Wang, J., McGuire, J.H., Burgdörfer, J. & Qiu, Y. (1996). *Phys. Rev. Lett.* **77**, 1723.
Wells, J.C., Schultz, D.R., Gavras, P. & Pindzola, M.S. (1996). *Phys. Rev. A* **54**, 593.